Original Article

Free Fatty Acids Produce Insulin Resistance and Activate the Proinflammatory Nuclear Factor-κB Pathway in Rat Liver

Guenther Boden,[1] Pengxiang She,[1] Maria Mozzoli,[1] Peter Cheung,[1] Kiranmai Gumireddy,[2] Prekumar Reddy,[2] Xiaqin Xiang,[3] Zhijan Luo,[3] and Neil Ruderman[3]

To study mechanisms by which free fatty acids (FFAs) cause hepatic insulin resistance, we have used euglycemic-hyperinsulinemic clamping with and without infusion of lipid/heparin (to raise or to lower plasma FFAs) in alert male rats. FFA-induced hepatic insulin resistance was associated with increased hepatic diacylglycerol content (+210%), increased activities of two serine/threonine kinases (protein kinase C-δ and inhibitor of κB [IκB] kinase-β), increased activation of the proinflammatory nuclear factor-κB (NF-κB) pathway (IκB kinase-β, +640%; IκB-α, −54%; and NF-κB, +73%), and increased expression of inflammatory cytokines (tumor necrosis factor-α, +1,700% and interleukin-1β, +440%) and plasma levels of monocyte chemoattractant protein-1 (+220%). We conclude that FFAs caused hepatic insulin resistance, which can produce overproduction of glucose and hyperglycemia, and initiated inflammatory processes in the liver that could potentially result in the development of steatohepatitis. *Diabetes* 54: 3458–3465, 2005

Obesity is closely associated with insulin resistance, type 2 diabetes, and the metabolic syndrome (also called the insulin resistance syndrome) (1). Obesity is also associated with increased presence in the circulation of several proinflammatory cytokines and chemokines and because of that has also been considered an inflammatory condition (rev. in 2). Whereas the reason for these associations is not entirely clear, it has been established that free fatty acids (FFAs) are a major link between obesity and insulin resistance/type 2 diabetes. This is based on the following evidence: most obese people have elevated plasma FFA levels, and FFAs cause insulin resistance dose dependently in skeletal muscle and liver (rev in 3). In skeletal muscle, FFAs inhibit insulin-stimulated glucose uptake at the level of glucose transport and/or phosphorylation (4,5) through mechanisms that involve intramyocellular accumulation of diacylglycerol (DAG) and long-chain acyl-CoA, activation of protein kinase C (PKC), and decreased tyrosine phosphorylation of insulin receptor substrate 1/2 (IRS-1/2) (6,7). The mechanisms by which FFAs cause hepatic insulin resistance have been directly addressed by only one study. In that study, Lam et al. (8) have shown that infusion of lipids (which increased plasma FFA levels) resulted in activation of PKC-δ in rat liver.

In the present study, we have used the lipid/heparin infusion to study effects of acutely elevated plasma FFA levels on insulin action in the rat liver. In this model, plasma FFA levels rise about equally in the systemic and the portal circulation. This is similar to the situation in postabsorptive, obese individuals who have ~80% of their fat in subcutaneous and intramuscular adipose tissue (releasing FFAs into the peripheral circulation) and ~20% of their fat in visceral adipose tissue (releasing FFAs at an increased rate into the portal circulation) (9,10).

RESEARCH DESIGN AND METHODS

Adult male Sprague-Dawley rats (250–300 g) were purchased from Charles River Laboratories (Wilmington, MA). They were housed in an environmentally controlled room with a 12-h light/dark cycle, where they had free access to standard rat diet (60% carbohydrate, 10% fat, and 30% protein) and water. One week before the studies, the animals were anesthetized with an intraperitoneal injection of phenobarbitol (50 mg/kg body wt). A polyvinyl catheter (internal diameter = 0.02 in) was inserted into the right internal jugular vein and extended to the right atrium. Another catheter was advanced through the left carotid artery until its tip reached the aortic arch. The free ends of both catheters were attached to long segments of steel tubing and tunneled subcutaneously to the back of the neck where they were exteriorized and secured to the skin with clips. At the end of the procedure, the catheters were flushed with isotonic saline containing heparin (40 units/ml) and Ampicillin (5 mg/ml) and filled with a viscous solution of heparin (300 units/ml) and 80% polyvinyl pyrolidone (PVP-10; Fisher Scientific, Pittsburgh, PA) to prevent refluxing of blood into the catheter lumen. All studies were performed in accordance with the guidelines for the use and care of laboratory animals of the Temple University Institutional Animal Care and Use Committee.

The rats were allowed 1 week to recover from the effects of surgery. At that time, they were within 3% of their preoperative weight. Euglycemic-hyperinsulinemic clamps were conducted in the morning after a 14-h overnight fast. Throughout the studies, the animals were allowed to move freely in their cages. All substrates were administered into the arterial catheter, and blood samples were obtained from the venous catheters. After the clamps, the rats were killed by on overdose of gaseous carbon monoxide and the livers freeze clamped, excised, and frozen at −80°C until assayed.

Euglycemic-hyperinsulinemic clamp study. Euglycemic-hyperinsulinemic clamps were performed with awake and unrestrained rats as described previously (11) with some modifications. Insulin (4.8 mU · kg^{-1} · min^{-1}) was

From the [1]Division of Endocrinology, Diabetes, and Metabolism, Temple University School of Medicine, Philadelphia, Pennsylvania; the [2]Fels Institute for Cancer Research and Molecular Biology, Temple University School of Medicine, Philadelphia, Pennsylvania; and the [3]Diabetes and Metabolism Research Unit, Boston University, Boston, Massachusetts.

Address correspondence to Guenther Boden, MD, Temple University Hospital, 3401 North Broad St., Philadelphia, PA 19140. E-mail: bodengh@tuhs.temple.edu.

Received for publication 22 June 2005 and accepted in revised form 25 August 2005.

AMPK, AMP kinase; DAG, diacylglycerol; EGP, endogenous glucose production; FFA, free fatty acid; GIR, glucose infusion rate; IκB, inhibitor of κB; IL, interleukin; IRS, insulin receptor substrate; MCP, monocyte chemoattractant protein; NF-κB, nuclear factor-κB; PKC, protein kinase C; ROS, reactive oxygen species; TNF, tumor necrosis factor.

infused through the jugular vein catheter from 0 to 240 min. Glucose concentrations were clamped at euglycemic levels by a variable rate infusion of 25% glucose. Blood glucose levels were monitored with an Elite Glucometer (Bayer, Elkhart, IN), and glucose infusion rates (GIRs) were adjusted every 5–10 min as needed.

HPLC-purified [3-^{3}H]glucose (NEC, Boston, MA) was infused through the jugular vein catheter (20-μCi bolus followed by 0.2 μCi/min from −100 to 0 min and 0.4 μCi/min from 0 to 240 min).

Liposyn II, a 20% triglyceride emulsion (Abbott Labs, Chicago, IL) was infused at 0.618 ml/h together with heparin (20 units/h). Controls received glycerol (143 μmol/h) instead of lipid/heparin. Glycerol was co-infused with insulin to match the glycerol content of Liposyn II.

Blood samples (~200 μl) were obtained from the carotid artery at −30, 0, 60, 120, 180, 210, and 240 min. Each blood sample was replaced by the same volume of fresh whole blood from a donor rat.

Glucose rates of appearance and disappearance. Glucose rates of appearance (G_{Ra}) were determined with [3-^{3}H]glucose as described previously (11). G_{Ra} and glucose rate of disappearance (G_{Rd}) were calculated using the non–steady-state equation of Steele et al. (12). The effective distribution volume for glucose was assumed to be 150 mg/kg.

Endogenous glucose production. Endogenous glucose production (EGP) was calculated as the difference between the isotopically determined G_{Ra} and the rate of glucose infused to maintain euglycemia (GIR).

$$EGP = G_{Ra} - \text{GIR}$$

Analytical procedures. Plasma insulin was measured in deproteinized serum by radioimmunoassay using rat insulin as standard (Linco, St. Charles, MO). FFAs were measured in plasma to which a lipoprotein lipase inhibitor (Paroxon; Sigma-Aldrich, St. Louis, MO) had been added with a kit from Wako Pure Chemicals (Richmond, VA).

Western analysis of PKC and IκB-α. PKC analysis was performed as described previously (6) with some modifications. In brief, frozen liver tissue was homogenized in 20 mmol/l Tris, pH 7.4, containing 10 mmol/l EDTA, 2 mmol/l EGTA, 100 mmol/l β-glycerophosphate, 0.05 mg/ml phenylmethylsulfonyl fluoride, 1 mg/ml leupeptin, and 0.1 mg/ml aprotinin. Samples were centrifuged in a Beckman air fuge at 160,000*g* for 20 min to separate the cytosolic fraction. The pellet was resuspended with the same homogenization buffer with 0.2% triton added, sonicated (Heat Systems Ultrasonics, Farmingdale, NY), and left on ice for 1 h. The homogenates were then recentrifuged, and the resultant supernatant was labeled as the membrane (particulate) fraction. Samples were loaded at a protein concentration of 50 μg/lane onto 8 and 12% SDS-polyacrylamide gels for PKC and IκB-α, respectively. PKC was determined in the cytosolic and membrane fractions, whereas IκB-α was determined in the cytosolic fraction only. Proteins were electrotransferred onto a polyvinylidene fluoride microporous membrane and isoform-specific polyclonal PKC or IκB-α antibodies (Santa Cruz Biotechnology, Santa Cruz, CA) at a dilution of 1:1,000 added to the membranes. Membranes were subjected to ECL reagent (Western blot chemiluminescence reagent; DupontNEN, Boston, MA). Multiple autoradiographs (to establish linearity) were quantitated using the NIH image analysis software (free distribution by National Institutes of Health [Bethesda, MD]). PKC-βI and -βII both ran as doublets when blotted with their respective antibodies. For purposes of comparison and because the two bands sometimes merged, both bands were included in the densitometric analysis.

PKC enzyme assay. PKC activity was determined as described elsewhere (6) using the PKC enzyme assay system (Amersham Life Science, Arlington Heights, IL). Liver was homogenized, and the cytosolic and particulate fractions were separated as described above. Samples were incubated at 37°C for 15 min. The phosphorylated peptide was separated using binding paper disks, and disks were counted for 10 min using Beckman LS 6500 (Beckman Instruments, Fullerton, CA).

DAG content. The measurement of DAG content was determined as described previously (13). In brief, lipids were extracted from liver samples using chloroform:methanol:PBS + 0.2% SDS (1:2:0.8). DAG kinase and [γ-^{32}P]ATP (15 μCi/μmol cold ATP) were added to extracts, and the reaction was stopped using chloroform:methanol (2:1). Samples were run on thin-layer chromatography plates in chloroform:acetone:methanol:acetic acid:water (100:40:20:20:10). The DAG bands were counted in a Beckman LS 6500 (Beckman Instruments).

IκB kinase immune precipitation and assay. Rat livers were homogenized in Nonidet P-40 lysis buffer containing 100 mmol/l HEPES (pH 7.6), 250 mmol/l NaCl, 10% glycerol, 1 mmol/l EDTA, 0.1% Nonidet P-40, and complete protease inhibitor cocktail. Lysates were clarified, and 200 μg was incubated with anti-IκB kinase (IKK-β) antibody from Santa Cruz Biotechnology (Santa Cruz, CA) for 4 h at 4°C. Then 50 μl protein A agarose was added to each of the immunoprecipitates and incubated for 2 h at 4°C. The immunoprecipitates were washed twice with PBS. In vitro kinase assays were performed with immune complexes in 20 μl kinase buffer containing 20 mmol/l Tris-HCl (pH 7.6), 10 mmol/l $MgCl_2$, 0.5 mmol/l dithiothreitol, 100 mmol/l ATP, 40 μCi [γ-^{32}P]ATP, and 2 μg glutathione S-transferase inhibitor of κB (IκB)-α or 1 μg histone H2B at 30°C for 20 min. Samples were analyzed by 15% SDS-PAGE and autoradiography.

Nuclear factor-κB activity. Total cell extracts were prepared and assayed for nuclear factor-κB (NF-κB) activities using a p65 assay kit (Active Motif, Carlsbad, CA) following the manufacturer's instructions. Ten micrograms total cell extract was incubated with NF-κB consensus oligonucleotide (5′-GGGACTTTCC-3′) at room temperature for 60 min, followed by incubation with anti-p65 antibody for 60 min and then with horseradish peroxidase-conjugated secondary antibody for 60 min. Absorption at 450 nm (A_{450}) was determined by spectrophotometry after color development. The specificity of the assay was verified by inhibition of the p65 activity of Jurkat cell nuclear extract by a wild-type NF-κB consensus oligonucleotide and noninhibition by a mutant oligonucleotide. A standard curve was constructed from the A_{450} versus protein concentrations of Jurkat cell nuclear extract (0.625, 1.25, 2.5, 5, and 10 μg). The relative binding activities in the total cell extracts of the frozen liver tissues were determined from the standard curve.

AMP kinase. The abundance of AMP kinase (AMPK), phosphorylated on threonine 172, was assayed with an antibody from Cell Signaling (Beverly, MA) as described previously (14).

Total RNA isolation and real-time RT-PCR. Total RNAs were isolated from frozen rat liver tissues by a modified method of Chomczynski and Sacchi (15) using a Rneasy kit (Qiagen, Valencia, CA). Real-time RT-PCR was performed with a SYBR Green One-Step qRT-PCR kit (Invitrogen, Carlsbad, CA) and a LightCycler (Roche, Indianapolis, IN). Primer sequences and reaction conditions for β-actin, tumor necrosis factor (TNF)-α, interleukin (IL)-6, and IL-1β were adapted from Peinnequin et al. (16). Standard curves of cycle threshold versus concentration were obtained using serial dilutions of a control rat liver total RNA. The crossing thresholds for β-actin were similar for the three groups of rats. Data were presented as a ratio of the relative concentration of the amplicon from sample after lipid or glycerol infusion versus that after saline infusion.

Monocyte chemoattractant protein-1. Monocyte chemoattractant protein (MCP)-1 was measured in rat serum using an Endogen Rat MCP-1 Elisa kit (Pierce Biotechnology, Rockford, IL).

Statistical analysis. All data are expressed as means ± SE. Statistical analysis was performed using the SigmaStat program (SPSS, Chicago, IL). ANOVA with repeated measures was used to determine the differences in G_{Rd} across time points. A Student's paired *t* test and paired nonparametric test (Wilcoxon's signed-rank test) for each time point were then performed if the overall comparison was statistically significant.

The difference between basal, glycerol, and lipid/heparin PKC activity and distribution, IκB-α abundance, and DAG were analyzed using the Student's unpaired *t* test and the Mann-Whitney Rank sum test (when the data were not normally distributed).

RESULTS

Euglycemic-hyperinsulinemic clamps. Plasma glucose in lipid/heparin and glycerol-infused (control) rats were clamped at mean concentrations of 5.4 ± 0.10 and 5.3 ± 0.09 mmol/l, respectively (Fig. 1*A*).

Serum insulin concentrations were raised from 54 ± 11 pmol/l to a mean clamp concentration of 430 ± 29 pmol/l in the lipid/heparin group and from 35 ± 6 to 440 ± 62 pmol/l in the glycerol (control) group (Fig. 1*B*).

Plasma FFA concentrations increased in the lipid/heparin group from 667 ± 29 to 2,374 ± 143 μmol/l ($P < 0.001$) and decreased in the glycerol controls from 624 ± 34 to 113 ± 12 μmol/l ($P < 0.001$) (Fig. 1*C*).

FFA-induced peripheral and hepatic insulin resistance. In response to hyperinsulinemia, the GIR needed to maintain euglycemia rose from 93 ± 1 to 178 ± 7 $\mu mol \cdot kg^{-1} \cdot min^{-1}$ in the glycerol controls ($P < 0.001$) by 1 h and then remained constant. In contrast, in the lipid/heparin group, an initial increase to 155 ± 3 $\mu mol \cdot kg^{-1} \cdot min^{-1}$ (at 60 min, $P < 0.01$) was followed by a decrease to baseline levels (88 ± 4 $\mu mol \cdot kg^{-1} \cdot min^{-1}$, $P < 0.01$) at the end of the study (4 h). GIR was significantly lower in the lipid/heparin compared with the glycerol controls between 90

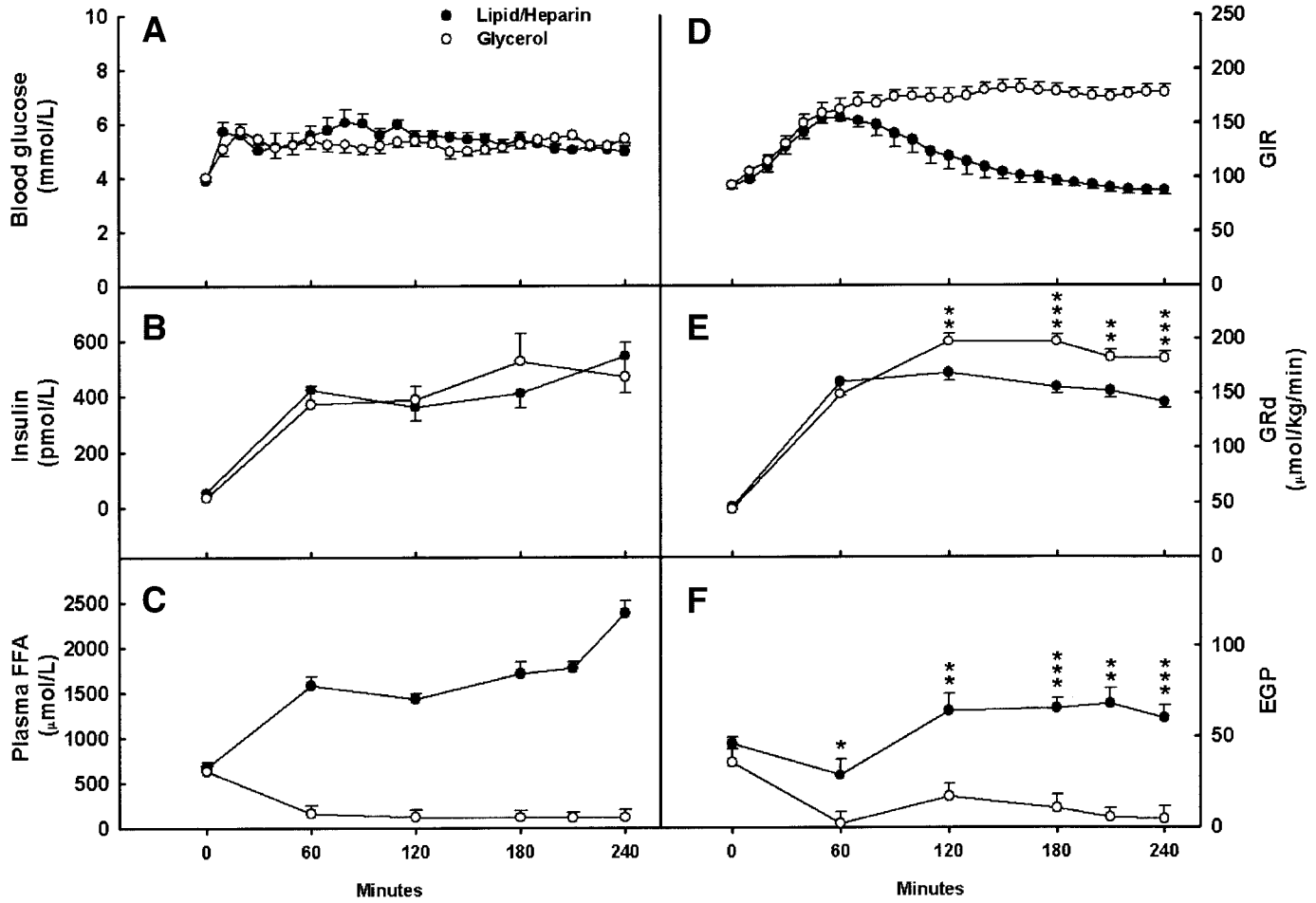

FIG. 1. Plasma glucose (*A*), insulin (*B*), and FFA (*C*) levels, GIRs needed to maintain euglycemia (*D*), GRds (*E*), and EGP rates (*F*) in eight adult male Sprague-Dawley rats during euglycemic-hyperinsulinemic clamping with either concurrent lipid/heparin or glycerol (control) infusions. Statistical analysis: *C* and *D*: $P < 0.01$ between 60 and 240 min comparing lipid/heparin versus glycerol infusions. *E* and *F*: *$P < 0.05$, **$P < 0.01$, ***$P < 0.001$ comparing lipid/heparin with glycerol infusions.

and 240 min (Fig. 1*D*). GIR is determined by two factors: *1*) the rate of glucose disappearance (G_{Rd}) and *2*) the rate of EGP (primarily from the liver).

G_{Rd} rose from 44 ± 2 (at 0 min) to 182 ± 3 μmol · kg^{-1} · min^{-1} (at 240 min) in the glycerol controls and from 46 ± 3 (at 0 min) to 142 ± 6 μmol · kg^{-1} · min^{-1} (at 240 min) in the lipid/heparin group ($P < 0.01$). G_{Rd} was significantly suppressed in the lipid/heparin compared with the glycerol controls between 120 and 240 min (Fig. 1*E*).

EGP increased from 46 ± 3 to 60 ± 5 μmol · kg^{-1} · min^{-1} in the lipid/heparin group and decreased from 44 ± 5 to 4 ± 7 μmol · kg^{-1} · min^{-1} in the glycerol controls. The differences between the two groups were highly significant between 60 and 240 min ($P < 0.001$) (Fig. 1*F*).

DAG, PKC, and AMPK. DAG concentrations in the liver increased from 96 ± 7 to 202 ± 26 pmol/mg wet tissue in the lipid/heparin group ($P < 0.001$) and did not change in the glycerol controls (96 vs. 82 pmol/mg wet tissue, NS) (Fig. 2*A*, *a*).

Total membrane-associated PKC activity increased from 439 ± 54 to 1,095 ± 195 arbitrary units (AU) in the lipid/heparin group ($P = 0.006$) and did not change in the glycerol controls (439 vs. 534 AU, NS) (Fig. 2*A*, *b*).

Translocation of PKC from the cytosol to the cell membrane is considered a sign of activation. PKC-δ–to–actin ratios decreased in the cytosol fraction (from 0.307 ± 0.02 to 0.199 ± 0.015, $P = 0.003$) and increased in the membrane fraction (from 0.406 ± 0.02 to 1.009 ± 0.03, $P < 0.001$) in the lipid/heparin group, whereas there were no significant changes in the glycerol controls (cytosol, 0.307 vs. 0.287, NS; membrane, 0.405 vs. 0.391, NS) (Fig. 2*A*, *c* and *d*).

There were no significant changes in cytosolic or membrane mass of the other PKC isoforms PKC-β1, PKC-βII, PKC-θ, or PKC-ζ in either group (Fig. 2*B*).

Decreases of ~20% in phosphorylated AMPK (threonine 172) from 16,310 ± 1,769 to 12,702 ± 1,890 AU during glycerol infusion and to 13,065 ± 947 AU during lipid/heparin infusion were not statistically significant. No independent effects of liposyn and heparin were found.

NF-κB pathway activity. IKK-β activity was 6.4-fold higher in the lipid/heparin group compared with noninfused rats (32,387 vs. 5,062 AU, $P = 0.002$). Hyperinsulinemia (glycerol controls) had no effect on IKK-β (5,062 vs. 5,488 AU) (Fig. 3*A*).

IκBα abundance decreased from 16,289 ± 2,472 to 7,432 ± 917 AU ($P = 0.035$) in the lipid/heparin group, whereas a smaller decrease in IκB-α in the glycerol controls from 16,289 to 12,117 was not statistically significant (Fig. 3*B*).

NF-κB activity was significantly higher in livers of lipid/heparin-infused rats than in livers of glycerol- or saline-infused rats (5.30 ± 1.1 vs. 3.34 ± 0.7 vs. 3.06 ± 0.27 AU, $P < 0.04$) (Fig. 3*C*).

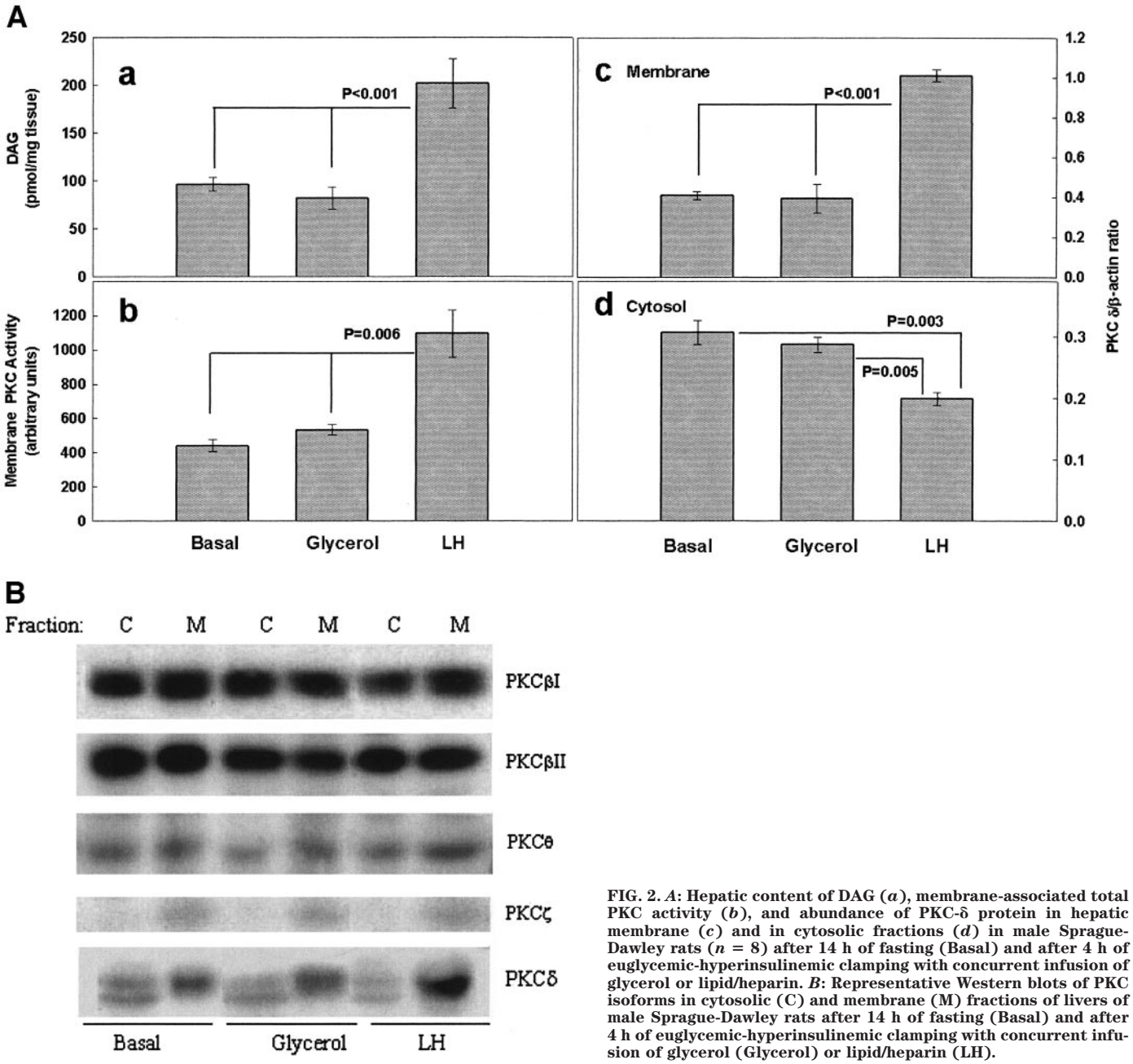

FIG. 2. *A*: **Hepatic content of DAG (*a*), membrane-associated total PKC activity (*b*), and abundance of PKC-δ protein in hepatic membrane (*c*) and in cytosolic fractions (*d*) in male Sprague-Dawley rats ($n = 8$) after 14 h of fasting (Basal) and after 4 h of euglycemic-hyperinsulinemic clamping with concurrent infusion of glycerol or lipid/heparin. *B*: Representative Western blots of PKC isoforms in cytosolic (C) and membrane (M) fractions of livers of male Sprague-Dawley rats after 14 h of fasting (Basal) and after 4 h of euglycemic-hyperinsulinemic clamping with concurrent infusion of glycerol (Glycerol) or lipid/heparin (LH).**

Expression of inflammatory cytokines. To assess effects of NF-κB activation on expression of inflammatory cytokines, we determined IL-1β, IL-6, and TNF-α mRNA by real-time RT-PCR in liver tissue (Fig. 4*A*). Lipid/heparin infusion increased the IL-1β–to–β-actin mRNA ratio 4.4-fold (basal 5.2 ± 1.8 vs. 23.2 ± 6.7 after lipid/heparin, $P < 0.03$) and the TNF-α–to–β-actin mRNA ratio 17.0-fold (basal 10.0 ± 4.8 vs. 170.9 ± 78.6 after lipid/heparin, $P < 0.05$). A 7.6-fold increase in the IL-6–to–β-actin mRNA ratio (basal 4.7 ± 1.9 vs. 35.9 ± 26.2) was not statistically significant. By comparison, hyperinsulinemia had no statistically significant effect on IL-1β, IL-6, or TNF-α.

Plasma MCP-1 levels. During lipid/heparin infusion, plasma MCP-1 levels rose 2.2-fold (from 8.2 ± 1.1 to 18.3 ± 4.3 ng/ml, $P < 0.05$), whereas plasma MCP-1 levels did not change during the glycerol infusions (6.4 ± 0.5 vs. 5.8 ± 0.9 ng/ml, NS) (Fig. 4*B*).

DISCUSSION

FFAs cause hepatic insulin resistance. In keeping with previous reports (17,18), we found that raising plasma FFA levels during euglycemic-hyperinsulinemic clamping inhibited hepatic insulin action after a delay of 1–2 h. The delay in the onset of FFA-induced insulin resistance in human and rat muscle was related to the slow but continuous accumulation in muscle cells of fat and intermediate metabolites of fatty acid esterification, including long-chain acyl-CoA and DAG (6,19). The development of insulin resistance in rat liver in the current study was similarly associated with an increase of hepatic DAG. Presumably, this occurred because DAG production, which in this setting is mostly due to esterification of 2-monoacylglycerol, exceeded DAG use. The high ambient insulin and glucose concentrations may have exaggerated this by inhibiting FFA oxidation (via increased formation

of malonyl-CoA), which would have increased the availability of cytosolic long-chain acyl-CoA for esterification (20).

Mechanism of FFA-mediated hepatic insulin resistance. The development of FFA-induced hepatic insulin resistance was associated with an increase in total membrane-associated PKC activity and translocation of PKC-δ from the cytosol to the cell membrane, which is considered a sign of activation. Because we found no cytosol to membrane translocation of other PKC isoforms, including PKC-β1, -β2, -θ, and -ζ (Fig. 2*B*), we believe that PKC-δ was responsible for most or all of the increased total membrane-associated PKC bioactivity.

Samuel et al. (7) have recently reported an increase in PKC-ε in livers of fat-fed rats. However, major differences in the experimental protocols (intravenous lipid/heparin infusion × 4 h, resulting in large increases in plasma FFAs in this study and the study by Lam et al. [8] vs. 3 days of fat feeding and no apparent changes in plasma FFAs in the Samuel study) make it difficult to compare the results of these studies.

The FFA-mediated increase in hepatic PKC activity was probably related to the increase in DAG, which is known to be a potent allosteric activator of conventional and novel PKC isoforms (21,22). In support of this notion, a linkage between DAG-associated PKC activation and insulin resistance has been found in skeletal muscle of humans and rodents in a wide variety of situations, including lipid infusion, fat feeding, obesity, denervation, and inactivity (6,23–25).

In addition to PKC-δ, FFAs also activated IKK-β, another serine/threonine kinase. IKK-β could have been activated via increased production of reactive oxygen species (ROS), because FFAs have been shown to increase ROS in endothelial cells in a PKC-dependent manner (probably by PKC-induced activation of NADPH oxidase) (26). Alternatively, IKK could have been directly activated by PKC (27,28).

Our demonstration that FFAs stimulated the activities of two different serine/threonine kinases is compatible with the widely held concept that an increase in serine phosphorylation of IRS-1/2 decreases tyrosine phosphorylation and by doing so interrupts insulin signaling, causing insulin resistance (7,29–31). IRS-1, however, has more than 40 serine/threonine consensus sites that can be phosphorylated (32), which makes this a rather complex issue. Thus, it is likely that still other kinases, for instance c-Jun NH_2-terminal kinase (7), are involved in phosphorylating some of these sites.

AMPK activity was not significantly diminished in the lipid or the glycerol infusion studies, suggesting that AMPK was not a factor involved in FFA-induced hepatic insulin resistance. In another study, one of us (N.R., personal communication) has found a 50% decrease in AMPK activity in Wistar rats during 6 h euglycemic-hyperinsulinemic clamps when plasma FFAs were increased by lipid infusion (33). Whether the length of the studies (4 vs. 6 h) or the different rat species (Sprague-Dawley versus Wistar) or the lipid infusion used account for the different findings is not clear.

Activation of the IKK/IκB/NF-κB pathway and transcription and secretion of proinflammatory cytokines. An important finding in this study was that FFA-induced insulin resistance was associated with activation of the proinflammatory NF-κB pathway. The 6.4-fold increase in IKK-β activity was accompanied by a large decrease (−50%) in IκB-α abundance and activation of NF-κB (as evidenced by an increase in DNA binding of its' p65 subunit). IκB is bound to NF-κB in the cytoplasm and inhibits its entrance into the nucleus. When phosphorylated by IKK-β or possibly other serine kinases such as PKC, IκB-α separates from the NF-κB complex and is ubiquitinated and degraded (34). This allows NF-κB to enter the nucleus where it induces the expression of genes responsible for synthesis of a number of inflammatory proteins (35). The changes in IKK-β, IκB-α, and NF-κB were accompanied by increased hepatic expression of several inflammatory cytokines (IL-1β, TNF-α, and IL-6) and by an increase in plasma MCP-1 levels, all known to be NF-κB–dependent inflammatory cytokines.

These findings may be relevant to the understanding of obesity-related steatohepatitis. Although the process remains poorly understood, hepatic insulin resistance and increased generation of inflammatory cytokines are currently considered important for the development of

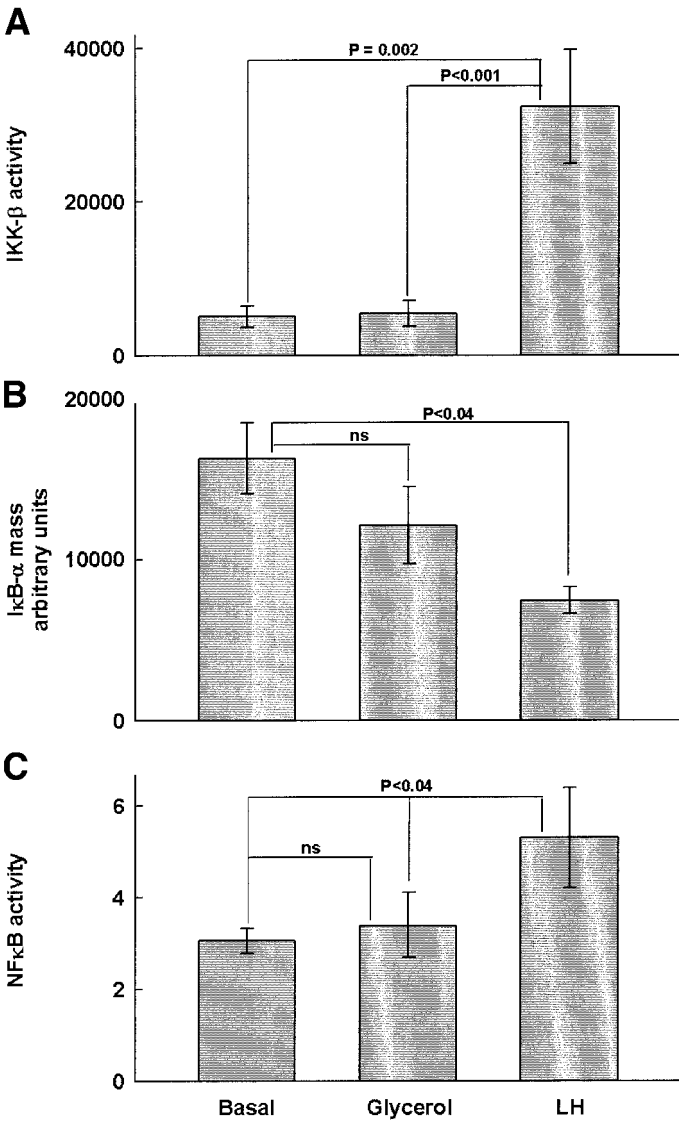

FIG. 3. IKK-β activity (*A*), IκB-α mass (*B*), and NF-κB activity (*C*) in livers of male Sprague-Dawley rats after 14 h of fasting (Basal, $n = 5$) and after 4 h of euglycemic-hyperinsulinemic clamping with infusion of glycerol ($n = 7$) or lipid/heparin (LH; $n = 7$).

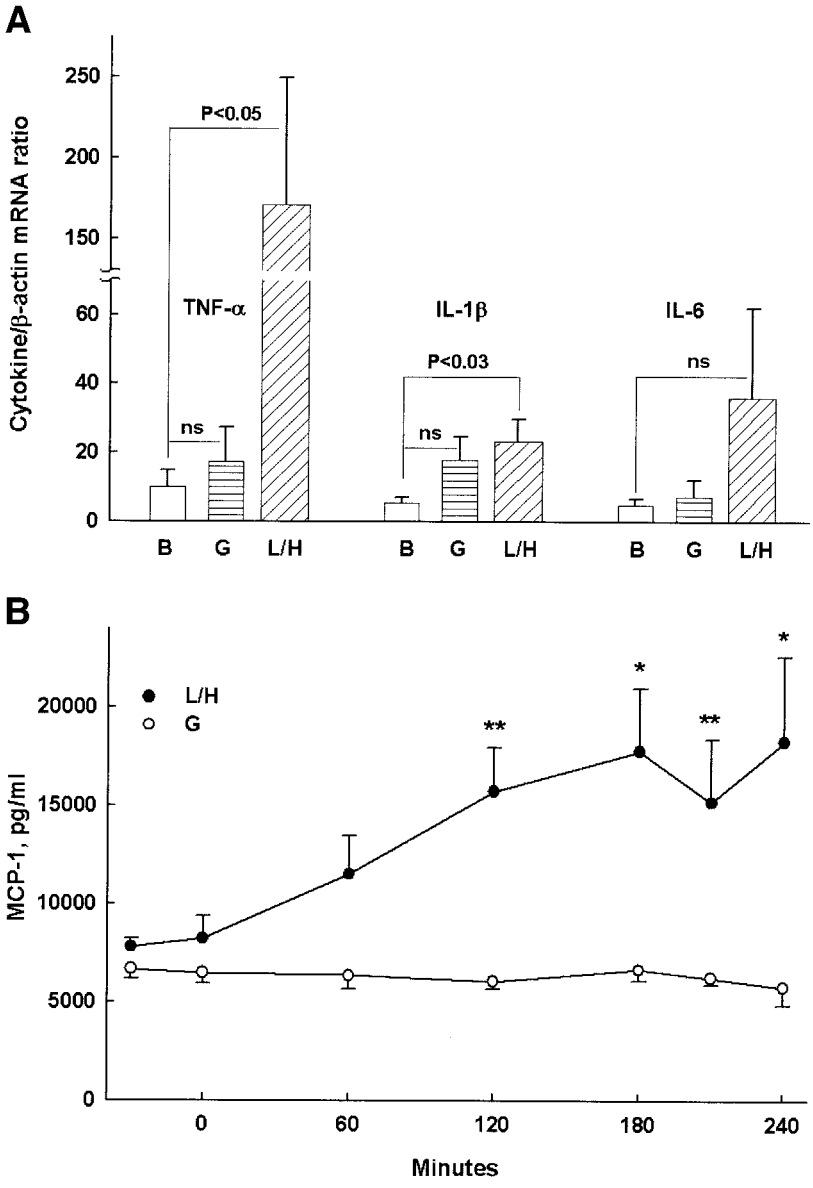

FIG. 4. *A*: **TNF-α, IL-1β, and IL-6 mRNA–to–β-actin ratios in livers of male Sprague-Dawley rats after 14 h of fasting (Basal [B], $n = 5$) and after 4 h of euglycemic-hyperinsulinemic clamping with infusion of glycerol (G; $n = 7$) or lipid/heparin (L/H; $n = 7$).** *B*: **Plasma MCP-1 concentrations during euglycemic-hyperinsulinemic clamping of overnight (14-h) fasted rats ($n = 6$).**

steatohepatitis (36,37). Our demonstration that acute elevation of plasma FFAs can cause acute hepatic insulin resistance and promote expression and production of inflammatory cytokines and chemokines via the IKK/IκB/NF-κB pathway suggested that FFAs may be able to initiate the development of steatohepatitis (Fig. 5).

Recently, Cai et al. (38) reported that mice fed a high-fat diet developed hepatic and systemic insulin resistance, hepatic steatosis associated with increased NF-κB activity, and subacute hepatic inflammation with increased production and secretion of several inflammatory cytokines. The same group had previously reported that IKK-β knock-out mice or treatment with aspirin in high doses (a nonspecific inhibitor of IKK) protected against development of insulin resistance in response to lipid infusions (39). Moreover, Arkan et al. (40) reported that loss of IKK-β in transgenic mice attenuated high-fat diet–induced hepatic insulin resistance and the expression and release of NF-κB–dependent inflammatory mediators.

These studies left unanswered the question as to how the high-fat diet caused hepatic insulin resistance and activation of NF-κB. The similarity between their and our results suggested, however, that FFAs might have been the mediator of the changes observed in the high-fat diet model. Nevertheless, our data are correlative and do not prove causality. Thus, the precise mechanisms by which FFAs activate the IKK/IκB-α/NF-κB pathway (via DAG/PKC, ROS, or other mechanisms) and how they cause insulin resistance, i.e., which of the many FFA-activated serine kinases are involved, remains to be determined.

In summary, we found that physiological elevations of plasma FFAs for 4 h caused hepatic insulin resistance (i.e., increased hepatic glucose production), resulted in hepatic accumulation of DAG, activation of two serine/threonine kinases (PKC-δ and IKK-β), activation of the classic proinflammatory IKK/IκB/NF-κB pathway, increased hepatic expression (IL-1β and TNF-α), and increased plasma levels (MCP-1) of inflammatory cytokines. These results suggested that obesity-associated hepatic insulin resistance and obesity-associated subacute hepatic inflammation could be the result of elevated plasma FFA levels.

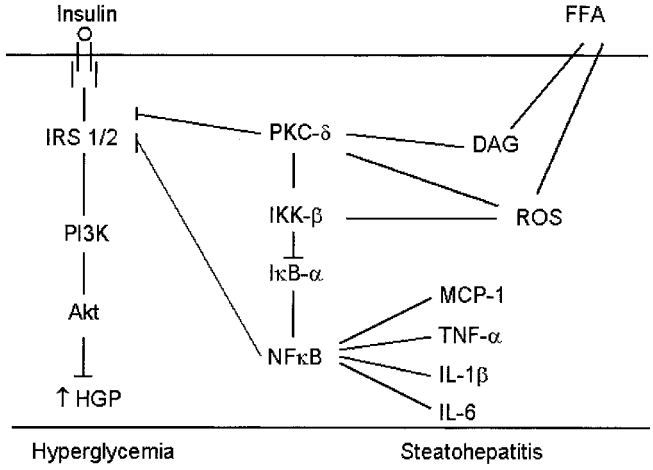

FIG. 5. Proposed scheme to explain the observed changes in response to hyperinsulinemia and elevated plasma FFAs. Key initiating events are *1*) hepatic accumulation of DAG and activation of serine/threonine kinases (PKC and IKK), which presumably caused insulin resistance at the IRS-1/2 level, and *2*) the activation of the IKK/IκB/NF-κB pathway (via PKC, ROS, or other mechanisms), leading to expression and secretion of inflammatory cytokines (TNF-α, IL-1, IL-6, and MCP-1) and, over time, development of hepatosteatitis.

ACKNOWLEDGMENTS

We thank Karen Kresge for outstanding technical assistance and Constance Harris Crews for typing the manuscript. We thank the Molecular Core Facility of the Center for Substance Abuse (grant no. P30-DA13429) for letting us use their Roche Light-Cycler for the real-time RT-PCR measurement.

G.B. has received support from National Institutes of Health Grants R01-AG-15353, R01-DK-58895, R01-HL-733267, and R01-DK-066003 and from a Mentor-Based Training Grant from the American Diabetes Association.

REFERENCES

1. Mokdad AN, Bowman BA, Ford ES: The continuing epidemics of obesity and diabetes in the United States. *JAMA* 286:1195–1200, 2001
2. Tataranni PA, Ortega E: A burning question: does an adipokine-induced activation of the immune system mediate the effect of overnutrition on type 2 diabetes? *Diabetes* 54:917–927, 2005
3. Boden G: Free fatty acids as target for therapy. *Curr Opin Endocrinol Diab* 11:258–263, 2004
4. Boden G, Chen X: Effects of fat on glucose uptake and utilization in patients with non-insulin-dependent diabetes. *J Clin Invest* 96:1261–1268, 1995
5. Dresner A, Laurent D, Marcucci M, Griffin ME, Dufour S, Cline GW, Slezak LA, Andersen DK, Hundal RS, Rothman DL, Petersen KF, Shulman GI: Effects of fatty acids on glucose transport and IRS-1 associated phosphatidylinositol 3-kinase activity. *J Clin Invest* 103:253–259, 1999
6. Itani SI, Ruderman NB, Schmieder, Boden G: Lipid-induced insulin resistance in human muscle is associated with changes in diacylglycerol, protein kinase C, and IκB-α. *Diabetes* 51:2005–2011, 2002
7. Samuel VT, Liu ZX, Qu X, Elder BD, Bilz S, Befroy D, Romanelli AJ, Shulman GI: Mechanism of hepatic insulin resistance in non-alcoholic fatty liver disease. *J Biol Chem* 279:32345–32353, 2004
8. Lam TKT, Yoshii H, Haber A, Bogdanovic Lam L, Fantus G, Giacca A: Free fatty acid-induced hepatic insulin resistance: a potential role for protein kinase C-δ. *Am J Physiol* 283:E682–E691, 2002
9. Mittleman SD, Van Citters GW, Kirkman EL, Bergman RN: Extreme insulin resistance of the central adipose depot in vivo. *Diabetes* 51:755–761, 2002
10. Chowdhury B, Sjostrom L, Alpsten M, Kostanty J, Kvist H, Lofgren R: A multicompartment body composition technique based on computerized tomography. *Int J Obes Relat Metab Disord* 18:219–234, 1994
11. Cheung P, Yang G, Boden G: Milrinone, a selective phosphodiesterase 3 inhibitor, stimulates lipolysis, endogenous glucose production, and insulin secretion. *Metabolism* 52:1496–1500, 2003
12. Steele R, Wall JS, DeBodo RC, Altszuler N: Measurement of size and turnover rate of body glucose pool by the isotope dilution method. *Am J Physiol* 187:15–24, 1956
13. Preiss J, Loomis CR, Bishop WR, Stein R, Niedel JE, Bell RM: Quantitative measurement of sn-1,2-diacylglycerols present in platelets, hepatocytes, and ras- and sis-transformed normal rat kidney cells. *J Biol Chem* 261:8597–8600, 1986
14. Tomas E, Tsao TS, Saha AK, Murrey HE, Zhang C, Itani SI, Lodish HF, Ruderman NB: Enhanced muscle fat oxidation and glucose transport by ACRP30 globular domain: acetyl-CoA carboxylase inhibition and AMP-activated protein kinase activation. *Proc Natl Acad Sci U S A* 99:16309–16313, 2002
15. Angulo P: Nonalcoholic fatty liver disease. *N Engl J Med* 346:1221–1231, 2002
16. Peinnequin A, Mouret C, Birot O, Alonso A, Mathieu J, Clarencon D, Agay D, Chancerelle Y, Multon E: Rat proinflammatory cytokine and cytokine related mRNA quantitation by real-time polymerase chain reaction using SYBR Green. *BMC Immunol* 5:3–12, 2004
17. Boden G, Cheung P, Stein TP, Kresge K, Mozzoli M: FFA cause hepatic insulin resistance by inhibiting insulin suppression of glycogenolysis. *Am J Physiol* 283:E12–E19, 2002
18. Boden G, Chen X, Ruiz J, White JV, Rossetti L: Mechanisms of fatty acid-induced inhibition of glucose uptake. *J Clin Invest* 93:2438–2446, 1994
19. Yu C, Chen Y, Cline GW, Zhang D, Zong H, Wang Y, Bergeron R, Kim JK, Cushman SW, Cooney GJ, Atcheson B, White MF, Kraegen EW, Shulman GI: Mechanism by which fatty acids inhibit insulin activation of insulin receptor substrate-1 (IRS-1)-associated phosphatidylinositol 3-kinase activity in muscle. *J Biol Chem* 277:50230–50236, 2002
20. Ruderman NB, Saha AK, Vavvas D, Witters LA: Malonyl-CoA, fuel sensing, and insulin resistance. *Am J Physiol* 276:E1–E18, 1999
21. Bronfman M, Morales MN, Orellana A: Diacylglycerol activation of protein kinase C is modulated by long-chain acyl-CoA. *Biochem Biophys Res Commun* 152:987–992, 1988
22. Nishizuka Y: Protein kinase C and lipid signaling for sustained cellular responses. *FASEB J* 9:484–496, 1995
23. Turinsky J, Bayly BP, O'Sullivan DM: 1,2-Diacylglycerol and ceramide levels in rat skeletal muscle and liver in vivo: studies with insulin, exercise, muscle denervation, and vasopressin. *J Biol Chem* 265:7933–7938, 1990
24. Bell KS, Schmitz-Peiffer C, Lim-Fraser M, Biden TJ, Cooney GJ, Kraegen EW: Acute reversal of lipid-induced muscle insulin resistance is associated with rapid alteration in PKC-theta localization. *Am J Physiol Endocrinol Metab* 279:E1196–E1201, 2001
25. Heydrick SJ, Ruderman NB, Kurowski TG, Adams HB, Chen KS: Enhanced stimulation of diacylglycerol and lipid synthesis by insulin in denervated muscle: altered protein kinase C activity and possible link to insulin resistance. *Diabetes* 40:1707–1711, 1991
26. Inoguchi T, Li P, Umeda F, Yu HY, Kakimoto M, Imamura M, Aoki T, Etoh T, Hashimoto T, Naruse M, Sano H, Utsumi H, Nawata H: High glucose level and free fatty acid stimulate reactive oxygen species production through protein kinase C-dependent activation of NAD(P)H oxidase in cultured vascular cells. *Diabetes* 49:1939–1945, 2000
27. Altman A, Isakov N, Baier G: Protein kinase C theta: a new essential superstar on the T-cell stage. *Immunol Today* 21:567–573, 2000
28. Kawakami Y, Nishimoto H, Kitaura J, Maeda-Yamamoto M, Kato RM, Littman DR, Rawlings DJ, Kawakami T: Protein kinase C βII Akt phosphorylation on Ser-473 in a cell type- and stimulus-specific fashion. *J Biol Chem* 279:47720–47725, 2004
29. De Fea K, Roth RA: Protein kinase C modulation of insulin receptor substrate-1 tyrosine phosphorylation requires serine 612. *Biochemistry* 36:12939–12947, 1997
30. Ravichandran V, Esposito DL, Chen J, Quon MJ: Protein kinase C-zeta phosphorylates insulin receptor substrate-1 and impairs its ability to activate phosphatidylinositol 3-kinase in response to insulin. *J Biol Chem* 276:3543–3549, 2001
31. Li Y, Nishimoto H, Kitaura J, Maeda-Yamamoto M, Kato RM, Littman DR, Rawlings DJ, Kawakami T: Protein kinase C θ inhibits insulin signaling by phosphorylating IRS1 at Ser^{1010}. *J Biol Chem* 279:45304–45307, 2004
32. Greene MW, Morrice N, Garofalo RS, Roth RA: Modulation of human insulin receptor substrate-1 tyrosine phosphorylation by protein kinase Cδ. *Biochem J* 378:105–116, 2004
33. Saha AK, Avilucea PR, Assifi MM, Kraegen EW, Ruderman NB: Pioglitazone treatment activates AMP-activated protein kinase in rat liver and adipose tissue in vivo. *Biochem Biophys Res Commun* 314:580–585, 2004
34. Karin M, Yamamoto Y, Wang QM: The IKK NFκB system: a treasure trove for drug development. *Nat Rev* 3:17–26, 2004

35. Barnes PJ, Karin M: Nuclear factor-kappaB: a pivotal transcription factor in chronic inflammatory diseases. *N Engl J Med* 336:1066–1071, 1997
36. Browning JD, Horton JD: Molecular mediators of hepatic steatosis and liver injury. *J Clin Invest* 114:147–152, 2004
37. Chomcznki P, Saacchi N: Single-step method of RNA isolation by acid guadinium thiocyanate-phenol-chloroform extraction. *Anal Biochem* 162: 156–159, 1987
38. Cai D, Yuan M, Frantz DF, Melendez PA, Hansen L, Lee J, Shelson SE: Local and systemic insulin resistance resulting from hepatic activation of IKK-β and NF-κB. *Nat Med* 11:183–190, 2005
39. Yuan M, Konstantopoulos N, Lee J, Hansen L, Li ZW, Karin M, Shoelson SE: Reversal of obesity- and diet-induced insulin resistance with salicylates or targeted disruption of Ikkbeta. *Science* 293:1673–1677, 2001
40. Arkan MC, Hevener AL, Greten FR, Maeda S, Li Z-W, Long JM, Wynshaw-Boris A, Poli G, Olefsky J, Karin M: IKK-beta links inflammation to obesity-induced insulin resistance. *Nat Med* 11:191–198, 2005